The effects of geometry on magnetic response of elliptical PHE sensors

Article *in* Journal of Applied Physics · June 2010

DOI: 10.1063/1.3337743 · Source: IEEE Xplore

Netanel Naftalis
Bar Ilan University

Doron Aurbach
Bar Ilan University

Lior Klein
Bar Ilan University

JOURNAL OF APPLIED PHYSICS **107**, 09E716 (2010)

The effects of geometry on magnetic response of elliptical PHE sensors

Isaschar Genish,[1,a)] Yishai Shperber,[1] Netanel Naftalis,[1] Gregory Salitra,[2] Doron Aurbach,[2] and Lior Klein[1]
[1]*Department of Physics, Nano-magnetism Research Center, Institute of Nanotechnology and Advanced Materials, Bar-Ilan University, Ramat-Gan 52900, Israel*
[2]*Department of Chemistry, Nano-magnetism Research Center, Institute of Nanotechnology and Advanced Materials, Bar-Ilan University, Ramat-Gan 52900, Israel*

(Presented 21 January 2009; received 2 November 2009; accepted 1 December 2009; published online 6 May 2010)

We present planar Hall effect measurements of elliptical permalloy sensors having different aspect ratios and thicknesses along with extensive numerical simulations and analytical analysis. We identify an upper limit for the sensor minor axis on the order of 1 μm above which hysteresis effects intensify. We also find that the increased ratio between the ellipse axes and thickness enhances the magnetic response of the sensor. © *2010 American Institute of Physics*.
[doi:10.1063/1.3337743]

I. INTRODUCTION

Magnetoresistive effects used in the fabrication of magnetic sensors include anisotropic magnetoresistance (AMR),[1] giant magnetoresistance,[2] tunneling magnetoresistance,[3] and planar Hall effect (PHE).[4] In all these cases the sensor consists of a magnetic film (or films) and the output signal is related to changes in the orientation of the internal magnetization. The sensitivity of such sensors depends on the magnitude of the magnetic response (namely, the change in magnetic orientation per given applied field and the magnetoresistance effect it produces) and on the magnetic noise.

The PHE and AMR are closely related phenomena manifested in transverse (ρ_{xy}) and longitudinal (ρ_{xx}) resistivities, respectively. In amorphous magnetic films the dependence of ρ_{xx} and ρ_{xy} on the angle θ between the current and the magnetization is given by

$$\rho_{xx} = \rho_{\perp} + (\rho_{\parallel} - \rho_{\perp})\cos^2 \theta, \tag{1}$$

$$\rho_{xy} = (\rho_{\parallel} - \rho_{\perp})\sin \theta \cos \theta. \tag{2}$$

Previous reports emphasized the intrinsic advantages of PHE sensors compared with other magnetoresistive sensors.[5,6] The advantages are in the convenient way of obtaining a linear response and in minimizing effects such as thermal drift which limits the sensitivity of AMR sensors. These features enabled the fabrication of high sensitivity PHE sensors[5] including sensors with magnetic flux concentrators which exhibit sensitivity in the range of nanotesla[6] and sensors whose sensitivity was demonstrated by measuring superparamagnetic spheres or magnetic dots with diameters of few microns.[7]

Here we explore how shape and size affect the behavior of elliptical PHE sensors. We do not address the field resolution of the sensors, but we concentrate on addressing how shape and size affect the magnetic response; the change in magnetic orientation and ranges of linear and reversible response. In this study, we compare measurements of fabricated sensors in the form of ellipse with numerical simulations (OOMMF) and theoretical models. We identify ranges of axis ratios and absolute sizes which yield better performance. The results may be used as guidelines for fabricating PHE sensors with higher sensitivity.

II. EXPERIMENTAL DETAILS

We use sputtered $Ni_{0.78}Fe_{0.22}$ films grown on silicone substrates. The films are 10 nm thick and they are capped with 3 nm of tantalum. The patterned sensors are fabricated by photolithography followed by electron beam lithography. Figure 1 shows one of the sensors whose measurements are reported here. It is composed of a magnetic ellipse with axes of 1.89 and 7.23 μm to which current and voltage leads made of gold are attached. The voltage leads are aligned across the ellipse to detect the PHE.

In this work we present measurements of two sensors in the form of ellipses with minor and major axes of 0.65 μm/2.44 μm and 0.83 μm/3.29 μm.

III. MEASUREMENTS

Figure 2 presents measurements of two sensors in the form of ellipses (0.65 μm/2.44 μm and

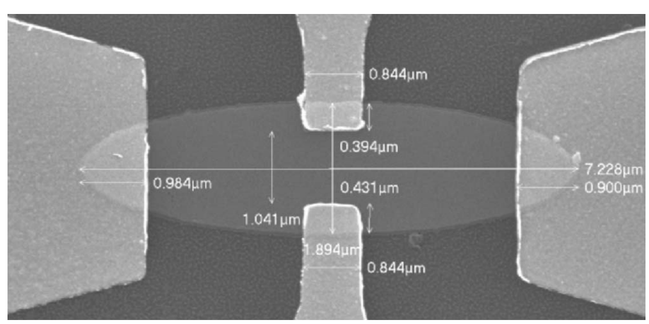

FIG. 1. A high resolution scanning electron microscope image of a PHE sensor.

a)Electronic mail: genishsi@biu.013.net.il.

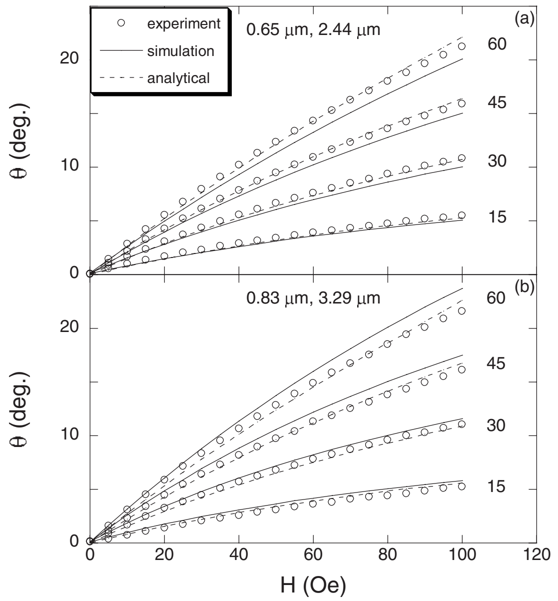

FIG. 2. The angle of the magnetization of sensors in the form of ellipse relative to the easy axis when an external field is applied at different angles (15°, 30°, 45°, and 60°) relative to the easy axis. The experimental results are given in circles. The continuous lines represent numerical simulations using OOMMF. The dashed lines represent the analytical solution of Eqs. (3) and (4). In (a) and (b) the results are from ellipses with dimensions of 0.65 μm/2.440 μm and 0.83 μm/3.29 μm, respectively.

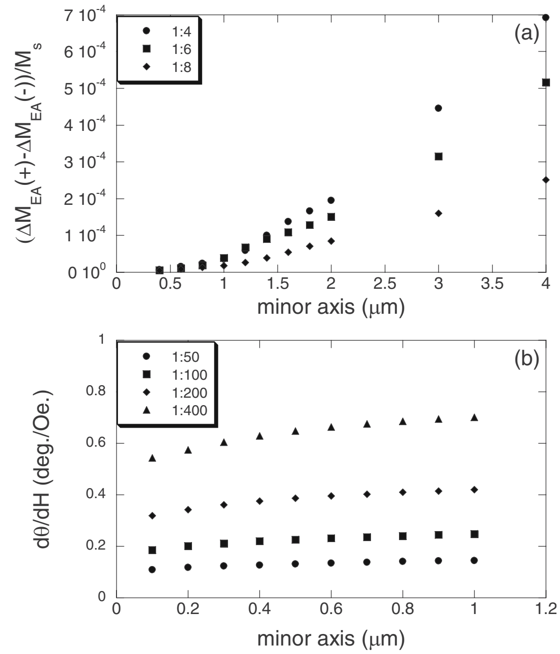

FIG. 3. (a) The difference in the induced magnetization for positive and negative fields (see text) for samples with different axis ratios: 1:4, 1:6, and 1:8. (b) The response of sensors for fields applied at 45° relative to the easy axis. The axis ratio of the sensors is 1:4 and the ratio between the film thickness and the minor axis varies between 1:50 and 1:400.

0.83 μm/3.29 μm). The measurements are performed by saturating the magnetization of the sensor along the long axis (easy axis) then the field is set to zero and a field is applied along different angles (15°, 30°, 45°, and 60°) relative to the easy axis. The angle θ of the magnetization is extracted from the PHE signal using Eq. (2).

We performed numerical simulations for samples of similar dimensions and composition using OOMMF. The initial state of the simulation is a random state, then a saturating field is applied along the easy axis and set to zero. At this stage a field is applied along the same angles as used in the experiment. The results of the simulations without any fitting parameters are represented in Fig. 2, showing a good agreement with the experimental results.

The behavior of the sensors can be described by the Stoner–Wohlfarth Hamiltonian that consists of an effective uniaxial anisotropy and a Zeeman term[8]

$$\mathcal{H} = K_u \sin^2 \theta - MH \cos(\alpha - \theta). \tag{3}$$

Here α and θ are the angles of the external field ($\mathbf{H}$) and the magnetization ($\mathbf{M}$) relative to the easy axis and K_u is the shape anisotropy constant. The response is determined by the ratio $M/2K_u$, where for a given angle θ, the angle α which minimizes the energy is determined by solving the equation

$$\sin \theta \cos \theta = H\frac{M}{2K_u}\sin(\alpha - \theta). \tag{4}$$

Using $M/2K_u$ as a free parameter, we can find a good fit to the experimental results (see Fig. 2).

The possibility to fit the experimental data with the Stoner–Wohlfarth Hamiltonian indicates that the fabricated sensors can be treated as single magnetic domains at least for a limited field range. We expect deviations from this behavior, and in the following we use numerical simulations to scan the effects of shape and size on the behavior of the sensors.

We start by using numerical simulations to examine the response of the sensor to positive and negative magnetic fields, where a difference in the response is an indication of a deviation from single-domain behavior. For this examination we fully magnetize the sensor from an initially random state with external field of 1000 Oe along its easy axis. After the stabilization of the magnetization we set the field to zero. Then we apply an increasing external field at 45° relative to the easy axis up to a maximum value of 2 Oe. To obtain the response of the sample to fields in opposite directions, we repeat this procedure with an external field oriented at 225° (instead of 45°) relative to the easy direction. For each of these simulations we calculate the change in the magnetization component along the easy axis relative to the initial remanent state ($\Delta M_{EA}^{+}/M_s$ for a field at 45° and $\Delta M_{EA}^{-}/M_s$ for a field at 225°). Subsequently, we calculate $\Delta M_{EA}^{+} - \Delta M_{EA}^{-}/M_s$. We performed these simulations for ellipses with axis ratios of 1:2, 1:3, 1:4, 1:6, and 1:8, and for each ratio we scanned a range of sizes of the short axis.

Figure 3(a) shows $\Delta M_{EA}^{+} - \Delta M_{EA}^{-}/M_s$ for different parameters. The results show that in general, this change increases as the size of the sample increases, and that for samples with minor axis larger than $\sim$1 μm this change starts increasing at a higher rate.

The response of the sensor is strongly affected by the ratio between the axes of the ellipse and the thickness. To explore the role of film thickness we perform simulations where we saturate sensors with length to width ratio of 1:4

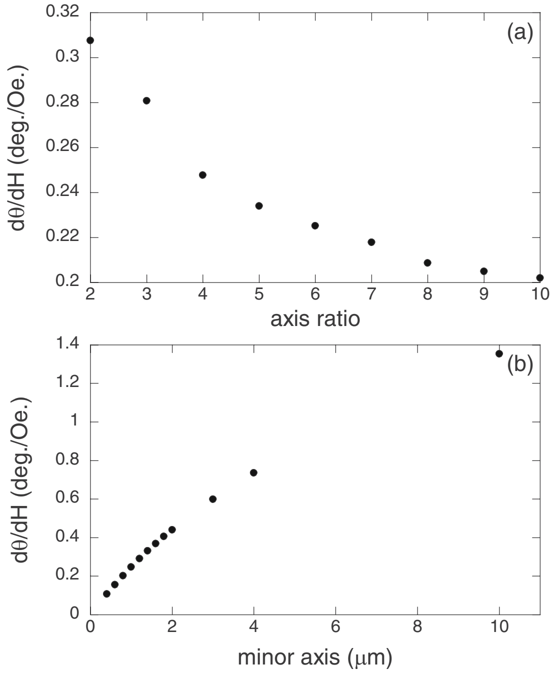

FIG. 4. (a) The response of sensors for fields applied at 45° relative to the easy axis as a function of axis ratio, where the minor axis is kept at 1 μm and the film thickness is 10 nm. (b) The response of sensors for fields applied at 45° relative to the easy axis. The axis ratio of the sensor is 1:4 and the film thickness is 10 nm.

and a minor axis in the range of 0.1–1 μm along the easy axis direction and then apply low external magnetic fields (up to 10 Oe) at 45° relative to the easy direction. The slope of $d\theta/dH$ that represents the response of the sensor was then extracted. Figure 3(b) shows the response determined as described. We see weak dependence on the length of the minor axis and strong dependence on the ratio between the minor axis and the thickness—the larger the ratio the stronger is the response.

Although it appears [Fig. 3(a)] that higher axis ratios yield more symmetric response, the response of the sensors decreases with increasing axis ratio. Figure 4(a) shows the response of ellipses with axis ratio between 1:2 and 1:10. The response is measured as in the previous experiments [Fig. 3(b)]. We note that changing the resistivity ratio by a factor of 5 (from 1:2 to 1:10) decreases the response of the sensor only by about 30%. On the other hand, changing the axis ratio by a factor of 2 [see Fig. 3(a)] can decrease the hysteresis quite significantly.

The simulations shown in Fig. 4(b) indicate that the higher the ratio between the minor axis and the thickness—the better. This can be achieved by decreasing the thickness or increasing the length of the minor axis. Concerning the thickness we can use films as thin as possible as long as we do not lose the AMR signal. Based on previous reports it means that we should use thicknesses in the range of 5–10 nm.[9] In order to obtain the highest ratio between the minor axis and the thickness we should use the largest minor axis possible without introducing hysteresis. Based on our simulations [Fig. 3(a)], it means we should use minor axis on the order of 1 μm. Using smaller minor axis is detrimental not only for the magnitude of the response, using too small sensors leads to the appearance of vortex states and the need for large saturating fields.

IV. CONCLUSIONS

We find a good fit between measurements, simulations, and analytical analysis of the behavior of ellipse shaped magnetic sensors. Based on this study we find that a large ratio between the ellipse size and thickness is important for high response. Nevertheless, there are limits to such increase since too thin films lose their PHE signal and too large minor axis introduces hysteresis. Based on our study we expect that sensors with axis ratio of 1:4–1:6 with thickness of 5–10 nm and minor axis size on the order of 1 μm may exhibit the best performance.

ACKNOWLEDGMENTS

We acknowledge the contribution of Omer Sinwani to numerical simulations. This research was supported by the Israel Science Foundation founded by the Israel Academy of Sciences and Humanities.

[1]I. A. Campbell, A. Fert and O. Jaoul, J. Phys. C **1**, S95 (1970); I. A. Campbell, Phys. Rev. Lett. **24**, 269 (1970); T. McGuire and R. Potter, IEEE Trans. Magn. **11**, 1018 (1975).
[2]M. N. Baibich, J. M. Broto, A. Fert, F. Nguyen Van Dau, F. Petroff, P. Etienne, G. Creuzet, A. Friederich, and J. Chazelas, Phys. Rev. Lett. **61**, 2472 (1988); G. Binasch, P. Grünberg, F. Saurenbach, and W. Zinn, Phys. Rev. B **39**, 4828 (1989); A. Fert, Rev. Mod. Phys. **80**, 1517 (2008).
[3]M. Julliere, Phys. Lett. **54**, 225 (1975); T. Miyazaki and N. Tezuka, J. Magn. Magn. Mater. **139**, 231 (1995); J. S. Moodera, L. R. Kinder, T. M. Wong, and R. Meservey, Phys. Rev. Lett. **74**, 3273 (1995).
[4]C. Goldberg and R. E. Davis, Phys. Rev. **94**, 1121 (1954); F. G. West, J. Appl. Phys. **34**, 1171 (1963); W. M. Bullis, Phys. Rev. **109**, 292 (1958).
[5]A. Schuhl, F. Nguyen Van Dau, and J. R. Childress, Appl. Phys. Lett. **66**, 2751 (1995); F. Nguyen Van Dau, A. Schuhl, J. R. Childress, and M. Sussiau, Sens. Actuators, A **53**, 256 (1996); F. Montaigne, A. Schuhl, F. Nguyen Van Dau, and A. Encinas, *ibid.* **81**, 324 (2000).
[6]F. Nguyen Van Dau, A. Schuhl, J. R. Childress and M. Sussiau, Transducers '95 * Eurosensors, 1995, Vol. 9, p. 241.
[7]L. Ejsing, M. F. Hansen, A. K. Menon, H. A. Ferreira, D. L. Graham, and P. P. Freitas, Appl. Phys. Lett. **84**, 4729 (2004); J. Magn. Magn. Mater. **293**, 677 (2005); K. M. Chui, A. O. Adeyeye, and M.-H. Li, *ibid.* **310**, e992 (2007).
[8]E. C. Stoner and E. P. Wohlfarth, Philos. Trans. R. Soc. London, Ser. A **240**, 599 (1948).
[9]Y. K. Kim and T. J. Silva, Appl. Phys. Lett. **68**, 2885 (1996); M. A. Akhter, D. J. Mapps, Y. Q. Ma Tan, A. Petford-Long, and R. Doole, J. Appl. Phys. **81**, 4122 (1997); D. A. Thompson, L. Romankiw, and A. Mayadas, IEEE Trans. Magn. **11**, 1039 (1975).